Dynamic enhancement of blast-resistant ultra high performance fibre reinforced concrete under flexural and shear loading

S.G. Millard, T.C.K. Molyneaux, S.J. Barnett, X. Gao

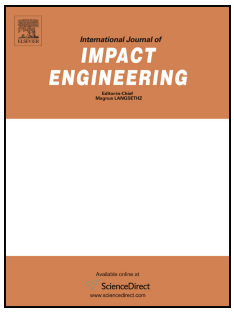

Title: Dynamic enhancement of blast-resistant ultra high performance fibre reinforced concrete under flexural and shear loading

Authors: S.G. Millard, T.C.K. Molyneaux, S.J. Barnett, X. Gao

PII: S0734-743X(09)00166-3

DOI: 10.1016/j.ijimpeng.2009.09.004

Reference: IE 1833

To appear in: *International Journal of Impact Engineering*

Received Date: 24 April 2009

Revised Date: 4 September 2009

Accepted Date: 17 September 2009

Please cite this article as: Millard SG, Molyneaux TCK, Barnett SJ, Gao X. Dynamic enhancement of blast-resistant ultra high performance fibre reinforced concrete under flexural and shear loading, International Journal of Impact Engineering (2009), doi: 10.1016/j.ijimpeng.2009.09.004

Dynamic enhancement of blast-resistant ultra high performance fibre reinforced concrete under flexural and shear loading

S.G. Millard [a] *, T.C.K. Molyneaux [b], S.J. Barnett [a], X. Gao [b]

[a] Department of Engineering, University of Liverpool, Liverpool, UK

[b] Department of Civil, Environmental and Chemical Engineering, RMIT, Melbourne, Australia

Abstract

Two independent projects are described in which drophammer techniques are used to investigate the dynamic increase factor (DIF) under both flexural and shear high-speed loading of a new ultra high performance fibre reinforced blast resistant concrete. The results from both studies correlate well. The results show that a DIF of the flexural tensile strength rising from 1.0 at 1 s^{-1} on a slope of 1/3 on a log (strain rate) versus log (DIF) plot can be used for design purposes. The results also show that no DIF should be used to increase the shear strength at high loading rates.

Keywords

Ultra high strength concrete, dynamic increase factor, fibre reinforcement, blast, bending, shear.

1. Introduction

Ultra high performance fibre reinforced concrete (UHPFRC) is a relatively new cementitious material[1], which has been developed to give significantly higher material performance than conventional concrete, fibre reinforced concrete (FRC) or engineered cementitious composites (ECC)[2]. A mix is designed to combine high cement content with a very low water/cement ratio. The selection of fine aggregates achieves maximisation of the particle packing density and minimises any localised non-homogeneity. Elevated temperature curing at 90 °C is also applied within the first week after casting. This process results in a very high compressive strength concrete, typically between 150-200 MPa. The addition of a high dosage of high tensile steel fibres, 13 mm in length and 0.2 mm diameter, results in a high flexural tensile strength, typically between 25-50 MPa. This material also

* Corresponding author. Tel: +44 151 794 5224.
E-mail address: ec96@liv.ac.uk (S.G. Millard).

has a very high capacity to absorb damage, with fracture energy in the range 20,000-40,000 J/m^2. UHPFRC has been commercially developed, e.g. *Ductal* [3]. Typical behaviour of UHPFRC under flexural testing is shown in Fig. 1 and this is compared with typical results for conventional plain concrete, FRC and ECC.

Normal reinforced concrete does not generally perform well under impact or explosion loading. An explosion adjacent to a concrete wall will cause a high-speed pressure wave to load the front face of the wall. A proportion of the energy will be reflected back and a significant proportion will propagate through the wall as a compressive stress wave. When this wave meets the back face of the wall there is another reflection with some of the energy returning through the wall and some propagating into the air. The reflection of the compressive stress wave within the concrete gives rise to a tension rebound from the back face. This can cause back face spalling as the concrete fails in tension and particles are ejected from the back surface at high speed, Fig. 2. As this failure normally occurs within the surface cover zone, the presence of conventional steel reinforcement will not help to control this event. It is thought that the high steel fibre content of the new UHPFRC material will help control back face spalling.

An explosive loading originating from a standoff location could cause failure in flexure of the entire concrete section[4], Fig. 3. An explosion occurring at a small standoff to the wall is likely to cause to a localised mode of failure, which can give rise to a shear-punching behaviour. The high inertial resistance of the wall can result in a localised failure before the body of the wall has time to respond to loading in a flexural mode. Localised back face spalling can still occur but a breach of the wall could occur due to a shear mode of failure[4], Fig. 4.

Impact of the wall by a high-speed object such as a bullet or explosion shrapnel has some similarities with a small standoff blast. Localised damage is likely on the front face and back face spalling can also occur. Dissipation of the impact energy can occur through ablation and deflection from hard inclusions within the concrete matrix (e.g. hard coarse aggregate particles). Shear friction and indirect tension can play a significant part in the failure mechanism[4].

It seems clear from the area under the load-deflection curve in Fig. 1 that UHPFRC should have good potential for absorbing energy through flexure. Furthermore studies of this material under dynamic loading have shown an increase in the ultimate strength with increasing strain rate[5, 6]. If the flexural tensile strength and fracture energy properties of UHPFRC can be shown to be enhanced at high strain rates then this material promises a high resistance to explosive loading giving rise to a flexural mode of behaviour. These material properties offer opportunities for using UHPFRC in blast resistant structures for applications such as antiterrorism and military defences.

As part of this study a series of full size UHPFRC panels have been subjected to blast loading at GL Industrial Services at the Spadeadam Test Site. Slabs with a height of 3.5 m were simply supported along their upper and lower edges and positioned at a relatively large standoff to induce a flexural mode of behaviour. It was observed that the response of these panels was impulsive, i.e. the high speed blast loading resulted in a much slower inertial flexural response of the panels. This typically showed a maximum tensile strain rate on the back face of the slabs in the region of 1 s^{-1}.

The properties of UHPFRC in flexural tension have not been investigated in detail, particularly at high strain rates. This paper reports on two independent investigations taking place simultaneously to characterise the material properties under impact loading using a drop-hammer facility. The results from studies conducted at RMIT, Melbourne, Australia are compared with results from a similar study conducted at the University of Liverpool, UK to determine the suitability of this UHPFRC to resist high strain rate impact loading, for strain rates in the region of 1 s^{-1}.

Several researchers have demonstrated that fibre reinforced concrete exhibits enhanced impact resistance compared to plain concrete[7, 8]. Fibre reinforced concrete subject to projectile impact has been observed to exhibit less damage than plain concrete[9, 10]. Maalej et al.[11] found that hybrid fibre reinforced concrete (using combinations of two or more types of fibres in the same concrete mixture) offered increased shatter resistance with reduced scabbing, spalling and fragmentation, whilst exhibiting better energy absorption. Gopalaratnam and Shah[8] investigated the effect of strain rates on the flexural properties of plain concrete and fibre reinforced concrete and concluded that fibre reinforced concrete is more rate-sensitive than plain concrete. The effect of strain rate on the tensile

strength of concrete has been examined by Malvar and Ross[12] who reported a dynamic increase factor (DIF) as high as 7. The flexural strength of fibre-reinforced concrete, regardless of fibre type and geometry, has been found to be greater under impact loading than under quasistatic loading by Bindiganavile & Banthia[13, 14]. A reduction in the energy absorption capacity of steel fibre reinforced concrete under impact loading was reported. In addition fibre pullout was observed to be the predominant mode of failure under both quasistatic and impact loading, although fracture of fibres became more common at higher strain rates.

2. UHPFRC Mix Development

UHPFRC has a cement or cementitious content over 3 times the content used in conventional concrete, typically in excess of 1000 kg/m^3. A high particle packing density can be achieved using no coarse aggregate and using fine silica sand with a typical particle size of 150-300 μm. At the University of Liverpool a high dosage of silica fume (SF), typically 10% by weight, with a typical particle size 100-500 nm, is used to create an optimised particle packing density and also for its pozzolanic properties. Some earlier research has investigated the replacement of some of the cement with ground granulated blast furnace slag (GGBS)[15]. It was reported that with GGBS levels of up to 35% of the total binder content, there was no detrimental effect on strength and workability was increased. GGBS has a particle size of < 20 μm and is a cementitious/pozzolanic material. A typical mix design for UHPFRC has been used/developed in the UK at the University of Liverpool and is shown in Table 1.

A similar UHPFRC mix was developed in Australia at RMIT. For reasons of commercial availability, silica fume manufactured as a byproduct of producing silicon metal or ferro-silicon alloys was replaced with Microsilica 600, a naturally extracted material having similar pozzolanic properties to silica fume and with a particle size in the range 1-10 μm. A typical mix design for UHPFRC developed at RMIT is shown in Table 2.

Similar short steel fibres (brass coated) were used in both investigations. However RMIT used a dosage of 1.5% by volume of concrete and the University of Liverpool investigated two mixes, one containing 2% steel fibres by volume of concrete and the other mix contained 6%. In addition a hybrid mix was also investigated at the University of Liverpool containing 3% of short fibres (13 mm length) and 3% of longer fibres (25 mm in length). It was thought that this hybrid fibre mixture would give an enhanced post-cracking behaviour.

Both universities employed an elevated temperature curing regime. At RMIT specimens were cured in water at 20 °C for a period of three days. Specimens were then heat treated in an oven at 160 °C for 24 hours. At the University of Liverpool specimens were cured under damp Hessian for 24 hours and were then conditioned at 90 °C in a hot water tank for six days.

3. Experimental Procedures

A series of static and dynamic tests were undertaken. These included

- Quasistatic compression testing-RMIT & Liverpool
- Quasistatic flexural testing-RMIT & Liverpool
- Quasistatic shear testing-Liverpool
- Dynamic flexural testing using a drophammer facility-RMIT & Liverpool
- Dynamic shear testing using a drophammer facility-Liverpool

3.1 Quasi static compression testing-RMIT & Liverpool

Static compression tests were undertaken at RMIT, using cylindrical 75 ×150 mm specimens. The demoulded specimens were longer than 150 mm, and the top surface was cut off to conform to the required 150 mm length using a diamond saw. Cylinders were not capped but covered by a pair of steel cavity plates containing rubber mats at each end.

At Liverpool specimens comprised 50 mm cubes. Static tests were conducted with a standard hydraulic testing machine at a loading rate of 20 MPa/min (RMIT) or 19.2 MPa/min (Liverpool).

3.2 Quasistatic flexural testing-RMIT & Liverpool

The RMIT beam specimens were 280 mm x 70 mm x 70 mm, with a span of 210 mm. Comparable Liverpool specimens were 350 mm x 100 mm x 50 mm high with a span of 300 mm. Although a size-effect has been observed for smaller specimens, related work at Liverpool showed that there is not a significant difference in flexural strength for beams of 100 mm and 50 mm height so it is not thought that the difference between the depths of the RMIT and Liverpool specimens would cause significant differences in test results. Specimens were orientated during testing so that the top and bottom beam surfaces were both smooth surfaces formed by the mould sides, i.e. the specimen was rotated through 90 degrees from its cast orientation. The quasistatic RMIT tests were conducted using a standard hydraulic testing machine with a constant loading rate of 0.26 kN/s, corresponding to a strain rate calculated by elastic bending theory of 6.8×10^{-6} s^{-1}. The Liverpool tests were similarly performed with a constant specimen deflection rate of 0.18 mm/min, corresponding to a strain rate on the soffit of the beam of 10^{-5} s^{-1}.

3.3 Quasistatic shear testing-Liverpool

Shear testing was carried out at Liverpool using small push-off specimens. These were designed to fail along a predetermined plane of weakness, Fig. 5. Specimens were cast on their side and had a shear area of 50 mm x 30 mm. Shear specimens were tested using a standard hydraulic compression test machine at a rate of 0.5 kN/s until the maximum load had been reached. The push-off specimens allowed a maximum shear deflection of 10 mm to be applied to the shear failure plane but during quasistatic loading this deflection limit was never reached.

3.4 Dynamic flexural testing using a drophammer facility-RMIT & Liverpool

3.4.1. RMIT drop-hammer tests

The drop-hammer facility developed at RMIT comprised a 30.1 kg cylindrical steel hammer, 2 m long with a diameter of 51 mm. The lower end of the hammer was hemispherical. The hammer was

lifted using a mechanical winch and released using an electrically operated magnetic release, Fig. 6a. The hammer was guided during its descent by projecting bolts and guide rails on either side. Flexural specimens for the dynamic testing were to the same specification as those used for quasistatic testing (Section 3.2).

The UHPFRC test beam was supported on two steel rollers and instrumented load cells. These load cells rested on a mass concrete slab, which was located on a 30 mm sand bed to reduce noise in the support load cells and transmission bar signals.

An impulse from the drop-hammer was transferred to the test beam using an instrumented transmission bar positioned centrally on top of the beam, Fig. 6b. A layer of fibreboard on top of the transmission bar was used to attenuate the deceleration force provided by the drop-hammer. By using a 15 mm layer of fibreboard, the instantaneous force transmitted by the drop-hammer was controlled and the event period increased, although the overall impulse remained invariant. The rate of loading was varied by changing the release height of the drop-hammer.

The natural frequency of the beams in the free-free mode is greater than 6000Hz (RMIT) and over 2000Hz (Liverpool). This resulted in the period of the response of the beam being significantly less than the period of loading and hence dynamic enhancement during these flexural tests not expected. This was confirmed by the output from the supporting load cells (only present in the RMIT tests) - these showed no indication of uplift or beam vibration response during the loading event. The use of fibre board to control the loading rate has the added advantage of providing damping and not exciting higher frequencies caused by ringing at impact. As a consequence the drop-hammer results at RMIT did not require filtering or smoothing. In addition data values were recorded at 10kHz which effectively removes any response above that frequency.

Interpretation of the drop-hammer test results was made more complicated because the rate of loading applied to the beam or shear specimens was not uniform. A typical result is shown in Fig. 7. It is seen from this figure that the rate of loading increases to a maximum value at around 7 kN, when cracking occurs. The loading rate then reduces until a peak load is reached. Results can be presented as a peak rate of loading, i.e. the maximum slope. Alternatively the mean rate of loading can be used as shown.

The rate of strain at the beam soffit was determined by using knowledge of the bending moment expected from mid-span loading of a simply-supported beam and Engineering Theory of Bending (i.e. plane sections remain plane). For the RMIT results the applied load together with an assumed elastic modulus of 35 GPa was used to evaluate the peak strain rate.

3.4.2. Liverpool drop-hammer tests

The Liverpool drop-hammer was developed on very similar principles to the RMIT facilities but used a lighter 23.3 kg hammer. The lighter hammer required the maximum release height of 2 m (corresponding to an impact speed of ~6 m/s) to be used throughout the entire test series to ensure complete failure of each specimen. The rate of loading was adjusted by using between 2 and 6 layers of 10 mm thick fibreboard between the hammer and the specimen to attenuate the rate of load transfer.

Flexural specimens for the dynamic testing were to the same specification as those used for quasistatic testing (Section 3.2).

Support reaction forces were measured using instrumented load cells developed in-house and positioned beneath the roller supports, Fig. 8. These load cells were located on a 50 mm thick steel base plate, which was itself located on a 10 mm layer of fibreboard to dampen out signal chatter. However a transmission bar was not used above the test beam to measure the applied impact force. Instead a laser Doppler anemometer (LDA) operating in reflection mode and focused on the drop-hammer itself was used to measure the speed time-history of the hammer. By differentiating the hammer speed with respect to time the acceleration and hence the force provided by the hammer could be evaluated. In addition a high-speed camera was used, with software referencing onto a high contrast target on the side of the test beam, to evaluate the beam displacement against time. Some signal filtering was required to smooth noise present, especially in the LDA speed measurements. Table 3 summarises the sampling frequencies used for data collection, as well as the signal filtering applied.

As verification of the test instrumentation, the hammer was dropped from a height of 1m onto a deep (non-yielding) steel beam. A comparison of the load applied to this steel beam measured using both the support load cells and the LDA facility showed a good agreement, although the laser instrumentation gave a noisier result, Fig. 9. In the case of a concrete beam tested to failure, this level

of agreement would not be expected since the inertial force and rotational effects are significant [16]. Further filtering can be used to smooth the laser results to give a better overall fit. Over-filtering however resulted in an unrealistic reduction in the measurement of the peak load.

For routine drophammer testing of concrete beams, LDA instrumentation was used to measure the velocity of the drophammer and the high-speed video facility was used to measure the deflection of the beam. The peak strain rate on the underside of the beam was determined from the deflection measurement. In one test to validate the accuracy of these two different instruments, both the LDA and the high-speed video facility were used to evaluate the velocity and displacement of the drophammer. This test was carried out with a drop height of 1 m and a calculated impact velocity of 4.4 m/sec was expected. The LDA results incorporated significant noise. However with appropriate filtering the velocities evaluated from the LDA and from the high-speed camera facility were reassuringly close, Fig. 10. In addition the velocity from both measurements was close to the expected value just before the drophammer impacted on the beam.

The results shown in Fig. 9 from a non-yielding steel beam can also be used to further validate the accuracy of the drop-hammer facility. The impulse provided by the drop-hammer is given by the area under the curve,

i.e. Impulse = $\int F.dt$

The area under the force vs time curve from the reaction load cells = 0.1111 kN.s

= **111.1 kg.m/s.**

However the impulse is also given by the change in momentum of the drop-hammer, i.e. hammer mass x change in velocity.

Impulse = 20 x (4.35-(-1.24)) = **111.8 kg.m/s**

For the Liverpool results, strain rate could be calculated either: i) from an applied load together with a measured elastic modulus, or ii) from the measured deflection. For comparability with RMIT the first method was used for subsequent analysis. The load used for calculating the strain rate was the load obtained from the support load cells. However in both cases once tensile cracking initiates then Engineering Bending Theory is no longer valid. From Fig. 11 it can be seen that the beam soffit strain determined from the beam deflection (as measured by the high speed camera) has some inbuilt

'noise' but quite closely follows the strain determined from the applied loading measured from the support load cells until a strain of about 0.0005 (500 με), when cracking first occurred. Beyond this point the beam deflection can no longer be used to determine the soffit tensile strain, since the beam is responding in a non-linear manner and is moving predominantly under its own inertia.

3.5 Dynamic shear testing

Shear specimens for the dynamic testing were to the same specification as those used for quasistatic testing (Section 3.3).A drop-hammer loading was applied to the top surface of the shear push-off specimens with the rate of loading again controlled by appropriate use of multiple layers of fibreboard. When failure occurred, the residual energy of the drop-hammer was absorbed by the single support load cell. Some specimens failed completely before the limiting shear displacement of 10 mm was reached while others still maintained some residual strength after 10 mm displacement, Fig. 12. However in all cases the peak shear strength was attained before 10 mm displacement.

The risk of accidentally overloading the load cell was significant and care had to be taken with the selection of suitable drop-hammer release height to prevent this happening. The nature of the stress distribution in the case of these shear specimens is not as straightforward as in the case of the beam specimens. Consequently the loading rate has been adopted as the parameter representative of strain rate. This is further discussed in Section 4 in the light of the results.

4. Test results

4.1. Static compression testing

Differences in the mix design and mixing and curing procedures used at RMIT and Liverpool resulted in a UHPFRC material with different compressive strengths. The RMIT static compressive strength was typically 125 MPa while compressive strength in the range of 180-200 MPa was achieved at Liverpool. This difference cannot be attributed to the small difference in cementitious content. Both UHPFRC mixes had almost the same water-cement ratio. It is thought that the different

curing procedure and the increased reactivity of the considerably finer silica fume instead of Microsilica 600 may have led to the increased compressive strength observed for the UHPFRC prepared at Liverpool. Typically silica fume comprises particles of size in the range 0.1-0.5 μm while the Microsilica particle size is 1-10 μm, an order of magnitude larger.

The difference in compressive strength resulting from an increase in fibre dosage from 2% to 6% at the University of Liverpool was relatively small and is also thought to be due to the increased density of the 6% mix rather than the effect of the fibres themselves. It is thought that the lower 1.5% dosage used by RMIT would not significantly influence the compressive strength. Additional tests at RMIT showed an insignificant difference in compressive strength between the 1.5% dosage and unreinforced specimens.

4.2. Static flexural testing

Table 4 shows the flexural strengths obtained from RMIT and Liverpool specimens. Increasing the level of steel fibre content resulted in an increase in the quasistatic flexural tensile strength. It can be see however that there are diminishing returns with increasing fibre content, with a threefold increase giving only a doubling in tensile strength. The RMIT and Liverpool results were consistent in the case of flexural strength. The lower value obtained for the RMIT specimens (which also had lower fibre content) is consistent with the observed trend.

4.3. Static shear testing

Increasing the level of steel fibre content also resulted in an increase in the maximum shear strength under quasistatic loading, as seen in Table 5. Shear failure resulted from a sliding friction action along the shear plane and pullout of the fibres in all cases.

4.4. Dynamic flexural testing

Typical results from the Liverpool dynamic flexural testing programme are shown in Fig. 13. Five replica beam specimens were tested using 6% steel fibres (by volume of concrete) and using 2 layers of 10 mm thick fibreboard to attenuate the impact. The maximum load sustained was between 30-38 kN, representing a maximum flexural tensile strength of 54-68 MPa. The fibreboard used for this series of tests gave a maximum strain rate of 1.66 s^{-1}. When these results are compared with the flexural tensile strength attained from quasistatic loading, a corresponding dynamic increase factor (DIF) of 1.51 was observed.

There was no significant variation in crack pattern or surface appearance observed for the different rates of loading and in all cases examined it was observed that pull-out was the only observed mode of failure for the fibres, even at higher strain rates.

The dynamic strength enhancement of all the Liverpool and RMIT test results is shown in Fig. 14. The results are compared with the models for strain rate enhancement of tensile strength of concrete proposed by Malvar and Ross [12] and Tedesco and Ross [17]. Malvar and Ross [12] proposed a formulation for the dynamic enhancement of concrete tensile strength as follows:

$$\frac{f_t}{f_{ts}} = \left(\frac{\dot{\varepsilon}}{\dot{\varepsilon}_s}\right)^{\delta} \qquad \text{for } \dot{\varepsilon} \le 1 s^{-1} \tag{1}$$

$$\frac{f_t}{f_{ts}} = \beta\left(\frac{\dot{\varepsilon}}{\dot{\varepsilon}_s}\right)^{1/3} \qquad \text{for } \dot{\varepsilon} > 1 s^{-1} \tag{2}$$

Tedesco and Ross [17] proposed the relationship:

$$\frac{f_t}{f_{ts}} = 2.929 \log \dot{\varepsilon} + 0.814 \le 6.0 \qquad \text{for } \dot{\varepsilon} > 2.32\ s^{-1} \tag{3}$$

$$\frac{f_t}{f_{ts}} = 0.1425 \log \dot{\varepsilon} + 1.833 \ge 1.0 \qquad \text{for } \dot{\varepsilon} \le 2.32\ s^{-1} \tag{4}$$

Where f_t = dynamic tensile strength at $\dot{\varepsilon}$

f_{ts} = static tensile strength at $\dot{\varepsilon}_s$

f_t / f_{ts} = tensile strength dynamic increase factor

$\dot{\varepsilon}$ = strain rate in the range of 10^{-6} to 160 s^{-1}

$\dot{\varepsilon}_s$ = 10^{-6} s^{-1} (static strain rate)

$$\log\beta = 6\delta - 2$$

$$\delta = 1/(1 + 8f'_c/f'_{co})$$

f'_{co} = 10 MPa

f'_c = concrete compressive strength, MPa

All the beam specimens show a significant DIF for strain rates between 0.1 and 10 s^{-1}. It can be seen that the dynamic increase factor is greatest for specimens without fibres and the enhancement effect is lower at higher fibre contents. The results obtained at RMIT for UHPFRC with 1.5% fibres are similar to those obtained at Liverpool for UHPFRC with 2% fibres. The dynamic increase factor is lowest for beams fabricated using a 6% blend of short and long steel fibres. The model based on the modified CEB formulation proposed by Malvar and Ross [12], given by equations (1) and (2), describes accurately the strain rate enhancement of UHPFRC with higher fibre contents. Neither of the models shown in the graph appears suitable for lower fibre contents although the Malvar and Ross relationship could be used as a conservative design DIF for all but the 6% hybrid fibre mixes. There is significant scatter observed from the results of the 6% hybrid fibre specimens. It is difficult to explain why some of these results show a DIF of less than 1.0. This is attributed to differences produced by either the mixing or testing methodology and is not thought to be significant. The standard error in the static flexural tensile strength of this mixture was 2.4 MPa (Table 4), significantly higher than the standard error obtained at lower fibre dosages. At strain rates above 1.0 s^{-1} the DIF for all the specimens can be described by the Malvar and Ross relationship for design purposes.

4.5. Dynamic shear testing

Fig. 15 demonstrates how the shear strength enhancement varies with loading rate when compared with the corresponding quasistatic shear strength. As discussed above, the shear stress loading rate is used because the assessment of the shear strain distribution in such a specimen is not clear. However, assuming an average shear stress based on the cross sectional area (50 x 30mm) an Elastic Modulus of 35GPa and a Poisson's Ratio of 0.2 then the peak shear strain rate tested is approximately 10 s^{-1}, corresponding to a loading rate of 2 x 10^5 kN/s. If a classic parabolic stress distribution is adopted this peak strain rate would increase to 15 s^{-1}. The results however indicate that there is no significant strain rate enhancement in the case of shear loading, which is a finding that is particularly significant when assessing the likelihood of punching failures.

The finding that there is insignificant shear strength enhancement for the rates tested is in line with the design advice offered in the widely used US army design guide [18], where an enhancement of only 10% is suggested in shear strength as opposed to 25% in flexural strength. In the flexural case the bending deformation is significant and the rise time of the loading in the case of short standoff events can often be less than the flexural periodic response. Hence the flexural strain rate experienced by a panel or beam will not be dependent on the rate of rise of the loading on the surface but on the response of the structure to the impulse (as observed in blast testing; Section 1). In the case of shear however the deformation and mass system is significantly stiffer and the rate of increase of the shear stress will reflect the rate of increase of the loading pulse. This can result in very high loading rates, above those tested here. Ongoing work is addressing this issue by testing specimens employing a Hopkinson bar facility.

5. Discussion

The flexural strength results show that the strain rate enhancement of flexural strength for UHPFRC is reduced as the fibre percentage increases from 0% to 6%. This can be explained by the time taken for micro crack propagation in the matrix. In unreinforced concrete in flexural tension the microcracks present in the structure grow as the stress increases. A microcrack will seek out the path

of lowest strength. This takes time and is a phenomenon well known and taken into consideration in concrete codes when specifying loading rates in standard testing of concrete samples. At higher loading rates the microcrack will not have time to develop laterally into regions of lower strength and will instead follow a more direct path through stronger regions. In fibre-reinforced beams, the fibres resist the lateral spreading of the cracks by bridging across regions of lower strength. Therefore, the beneficial effect of a restraint on lateral crack growth has already been partially accounted for by fibre reinforcement, resulting in higher failure strength under quasistatic loading. Subsequently, the influence of the higher loading rate on reducing lateral crack development would be lessened. The UHPFRC using hybrid fibres shows a lesser DIF than the mixes using only shorter fibres. This is attributed to the improved efficiency of hybrid steel fibres of different lengths in controlling the development of lateral crack growth at low strain rates.

The observation that DIF reduces for higher fibre content contradicts an earlier study [8] on FRC of a more conventional compressive strength. However it is consistent with previous observations that high-strength concrete has a lower strain rate sensitivity[12]. In addition, the mode of failure of UHPFRC is invariably one of fibre pullout, due to the very short (13 mm) length of fibres used. Pullout of straight fibres has previously been shown to be independent of strain rate[19].

The implications for design under blast and impact loading are that for flexural strain rates of less than 1 s^{-1} no DIF should be used. 1 -100 s^{-1} is a strain rate typical for concrete subjected to conventional military weapons [16]. 1 s^{-1} was measured by the Authors for a wall structure under blast loading at large standoff, see Section 1.0. Flexural loading producing a tensile strain rate above 1 s^{-1} will enable a DIF to be used in design. A DIF rising from 1.0 at 1 s^{-1} on a slope of 1/3 on a log (strain rate) versus log (DIF) plot has been proposed [12] for conventional plain concrete and is shown on Figure 14. This DIF appears to be suitable or conservative for all UHPFRC containing single size 13 mm fibres. This is applicable to a wide range of mixes and fibre content (1.5-6.0%). A typical fibre content in UHPFRC structural members is in the range 1.5-2.0%. Within the larger experimental scatter, this DIF function also looks as though it could also be appropriate for UHPFRC using a 6% hybrid of short and long fibres. At higher rates of strain (> 5 s^{-1}) this enhancement

exceeds that recommended for conventionally reinforced concrete in the US Army design guidelines TM 5-1300[18] which advises an enhancement in the range 19-25% (for large and small stand-off).

The implication of these finding in terms of the appraisal of shear resistance is that it would not be appropriate to apply any enhancement when evaluating the resistance to punching shear, expected to be the principal mode of failure at short standoff.

6. Conclusions

The results of two independent studies at the University of Liverpool in the UK and at RMIT in Australia on UHPFRC have shown that under flexural loading at the high rates of strain of 1.0 s^{-1} and above that might be expected under large standoff blast wave or impact loading, a dynamic increase factor of the flexural tensile strength rising from 1.0 at 1 s^{-1} on a slope of 1/3 on a log (strain rate) versus log (DIF) plot (Equation (2) [12]) can be used for design purposes.

It was found from studies of the shear behaviour that at high shear stress loading rates of up to 120 MPa/s, no significant dynamic increase factor was observed. Shear is expected to be the dominant mode of behaviour of UHPFRC under blast loading at close standoff. Hence no strain rate enhancement is recommended when designing a blast resistant UHPFRC for shear punching resistance.

The wide range of steel fibre content and differences in UHPFRC mix constituents used in the two studies did not have any significant influence on the above findings.

7. Acknowledgements

The University of Liverpool study has been carried out with the support of the UK Engineering and Physical Sciences Research Council under the “Think Crime – 4” Managed Programme (Grant

number EP/D041201/1). We would like to thank the following companies for supply of materials and technical assistance: Bekaert, Fosroc, Elkem, Castle Cement, Appleby Group.

The RMIT study was carried out as part of an internally funded study in the School of Civil, Environmental and Chemical Engineering.

8. References

1. Richard P, Cheyrezy M. Composition of reactive powder concretes. Cem Concr Res 1995; 25(7): 1501-1511.
2. Li VC, Kanda T. Engineered cementitious composites for structural applications. J Mat Civil Engng 1998; 13(4): 66-69.
3. Behloul M, Durukal A, Batoz J-F, Chanvillard G. Ductal: ultra high-performance concrete technology with ductility. In: Di Prisco M, Felicetti R, Plizzari GA, editors. Proceedings of 6th RILEM Symposium on Fibre-Reinforced Concretes (FRC). Varenna, Italy: RILEM Publications S.A.R.L., 2004. p. 1281-1290.
4. Smith PD, Hetherington JG. Blast and Ballistic Loading of Structures. Oxford: Butterworth-Heinemann, 1994.
5. Tai Y-S. Dynamic compressive characteristic of reactive powder concrete under various loading rates. In: Banthia N, Mindess S, Fujikake K, editors. Proceedings of PROTECT2007: Performance, Protection and Strengthening of Structures under Extreme Loading. Whistler, BC, Canada, 2007.
6. Toutlemonde F, Boulay C, Sercombe J, Le Maou F, Renwez S, Adeline R. Characterization of reactive powder concrete (RPC) in direct tension at medium to high loading rates. In: Gjørv O, Sakai K, Banthia N, editors. Proceedings of Concrete under Severe Conditions 2: Environment and Loading. Tromsø, Norway: E&FN Spon, 1998. p. 887-896.
7. Banthia N, Mindess S, Trottier J-F. Impact resistance of steel fiber reinforced concrete. ACI Mater J 1996; 93(5): 472-479.
8. Gopalaratnam VS, Shah SP. Properties of steel fiber reinforced concrete subjected to impact loading. J Am Concr Inst 1986; 83(1): 117-126.
9. Dancygier AN, Yankelevsky DZ, Jaegermann C. Response of high-peformance concrete plates to non-deforming projectiles. Int J Impact Engng 2007; 34(11): 1768-1779.
10. Luo X, Sun W, Chan SYN. Characteristics of high-performance steel fiber-reinforced concrete subject to high velocity impact. Cem Concr Res 2000; 30(6): 907-914.

11. Maalej M, Quek ST, Zhang J. Behavior of hybrid-fiber engineered cementitious composites subjected to dynamic tensile loading and projectile impact. J Mat Civil Engng 2005; 17(2): 143-152.

12. Malvar LJ, Ross CA. Review of strain rate effects for concrete in tension. ACI Mater J 1998; 95(6): 735-739.

13. Bindiganavile V, Banthia N. Polymer and steel fiber-reinforced cementitious composites under impact loading. ACI Mater J 2001; 98(1): 10-16.

14. Bindiganavile V, Banthia N. Polymer and steel fiber-reinforced cementitious composites under impact loading - Part 2: Flexural toughness. ACI Mater J 2001; 98(1): 17-24.

15. Le TT, Soutsos MN, Millard SG, Barnett SJ. UHPFRC - Optimisation of mix proportions. In: Russell MI, Basheer PAM, editors. Proceedings of Concrete Platform. Belfast: Queen's University of Belfast, 2007. p. 339-348.

16. Banthia N, Mindess S, Bentur A, Pigeon M. Impact testing of concrete using a drop-weight impact machine. Experimental Mechanics 1989; 29(1): 63-69.

17. Tedesco JW, Ross CA. Strain-rate-dependent constitutive equations for concrete. Journal of Pressure Vessel Technology 1998; 120(4): 398-405.

18. Joint Departments of the Army, the Navy and the Air Force. Structures to resist the effects of accidental explosions. TM 5-1300/NAVFAC P-397/AFR 88-22 Washington DC. 1990.

19. Gokoz UN, Naaman AE. Effect of strain-rate on the pull-out behaviour of fibres in mortar. International Journal of Cement Composites 1981; 3(3): 187-202.

Figure Captions

Table 1

University of Liverpool UHPFRC mix proportions

Cementitious component (kg/m^3)				Aggregate sand (kg/m^3)	Water-binder ratio	Structuro 11180 Superplasticiser (*l*)
Cement	GGBS (level of cement replacement)	SF	Total (C+GGBS+SF)			
657	418 (35%)	119 (10%)	1194	1051	0.17	40

Table 2

RMIT UHPFRC mix proportions

Cementitious component (kg/m^3)			Aggregate sand (kg/m^3)	Water-binder ratio	Glenium 51 Superplasticiser (*l*)
Cement	Microsilica 600 (level of cement replacement)	Total (C+ SF)			
955	143 (15%)	1098	1100	0.153	60

Table 3

Data collection and filtering frequencies

Measurement	Data collection rate (kHz)	Filtering (kHz)
Load cells	250	1
Laser Doppler anemometer	~130	0.5
High speed camera	6	N/A

Table 4

Static flexural tensile strength

Fibre content (% by volume)	Flexural tensile strength (MPa)	Standard error (MPa)
1.5	21.9	0.6
2.0	25.0	0.5
6.0	45.8	2.0
6.0 - hybrid	53.6	2.4

Table 5

Quasistatic shear strength

Fibre content (% by volume)	Shear strength (MPa)	Standard error (MPa)
1.5	-	-
2.0	24.6	3.0
6.0	38.3	0.3
6.0 – hybrid	38.6	1.1

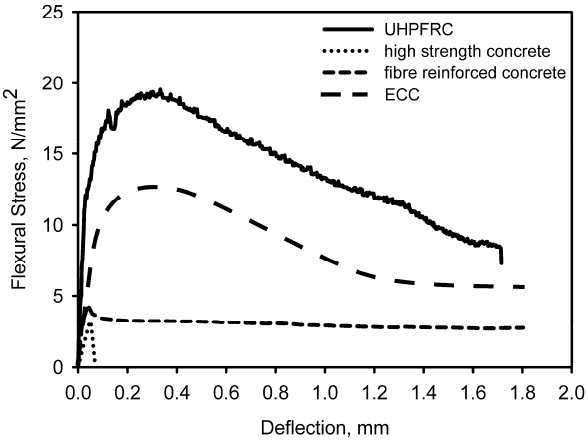

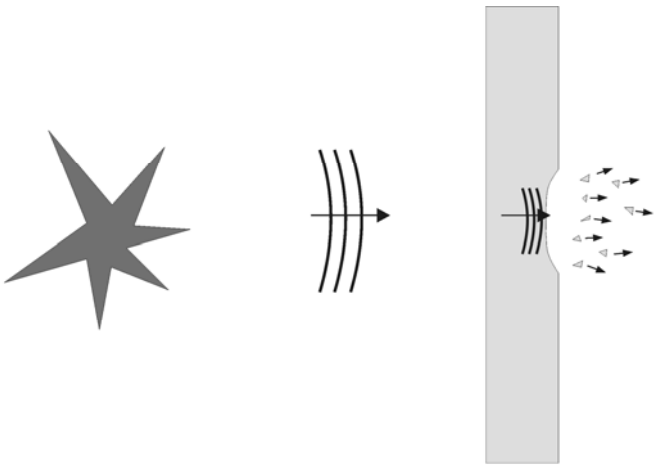

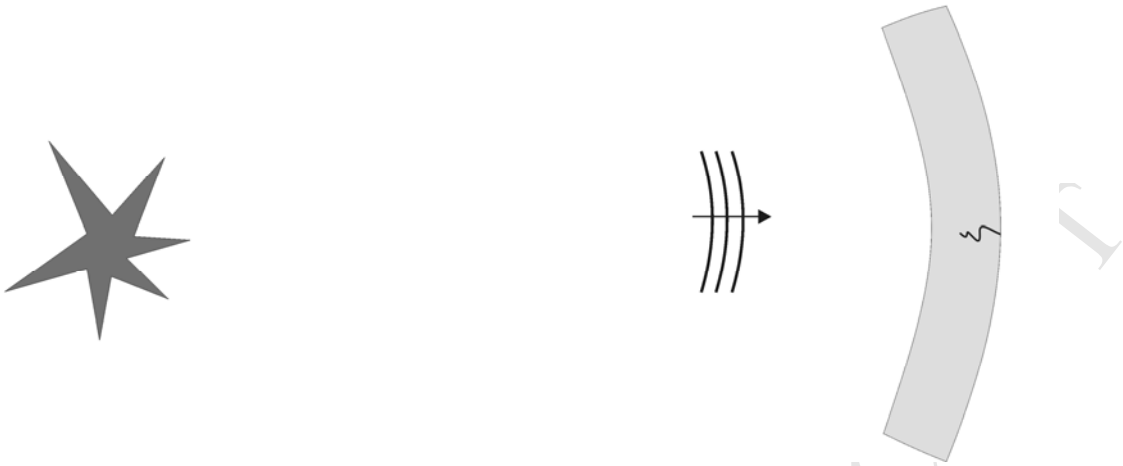

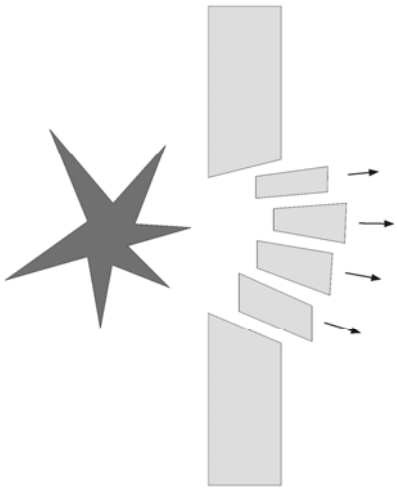

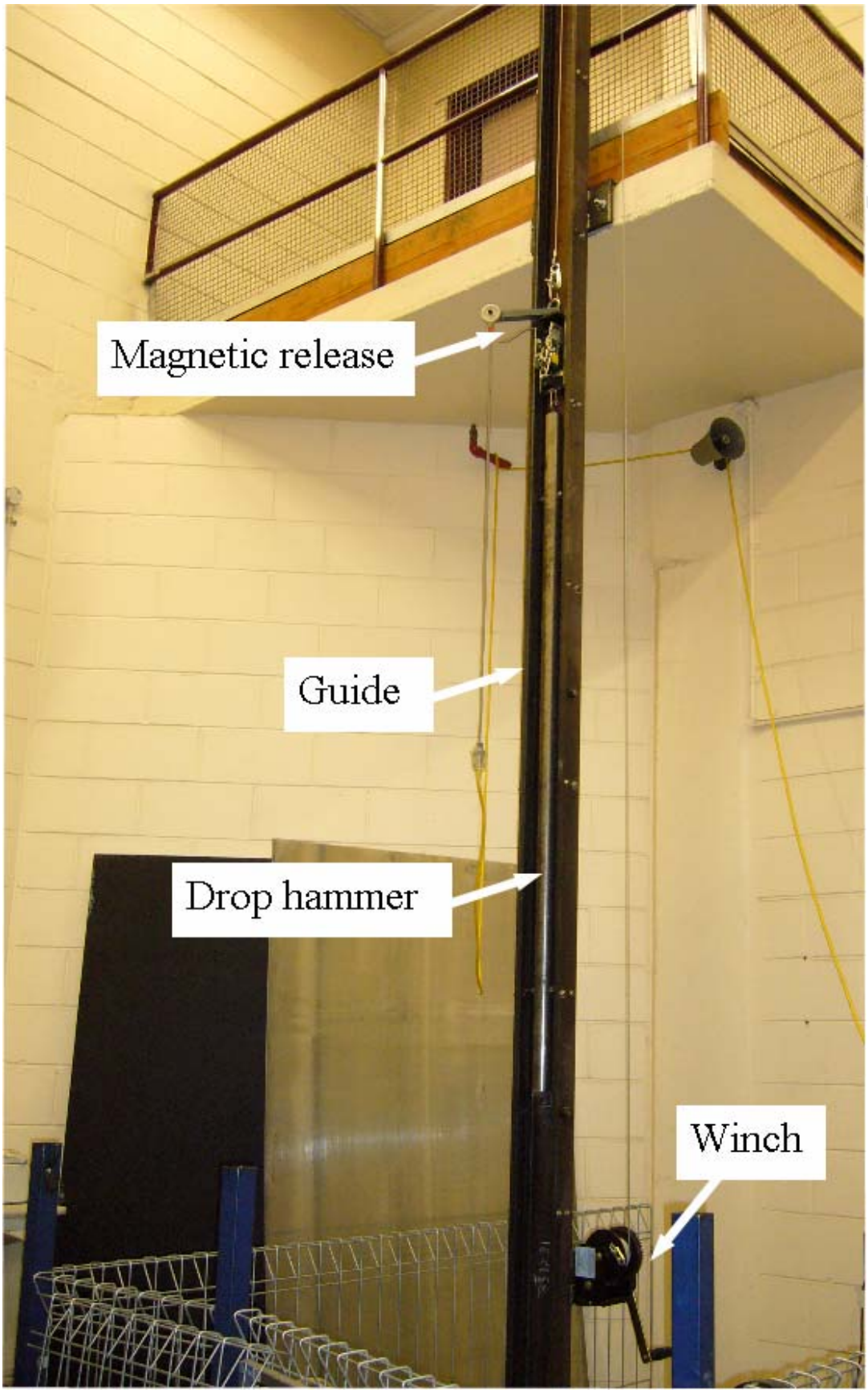
Magnetic release
Guide
Drop hammer
Winch

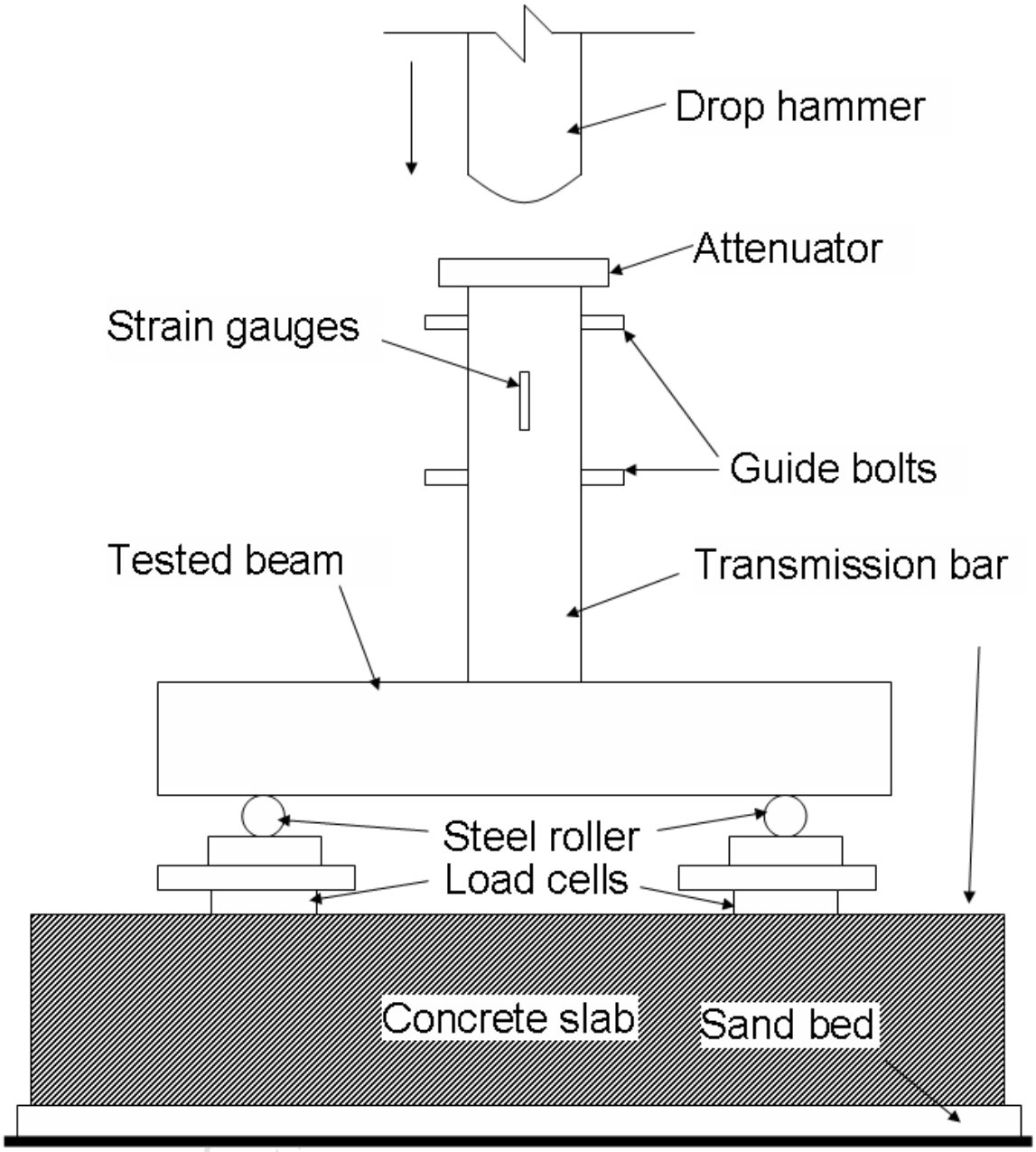
Drop hammer
Attenuator
Strain gauges
Guide bolts
Tested beam
Transmission bar
Steel roller
Load cells
Concrete slab
Sand bed

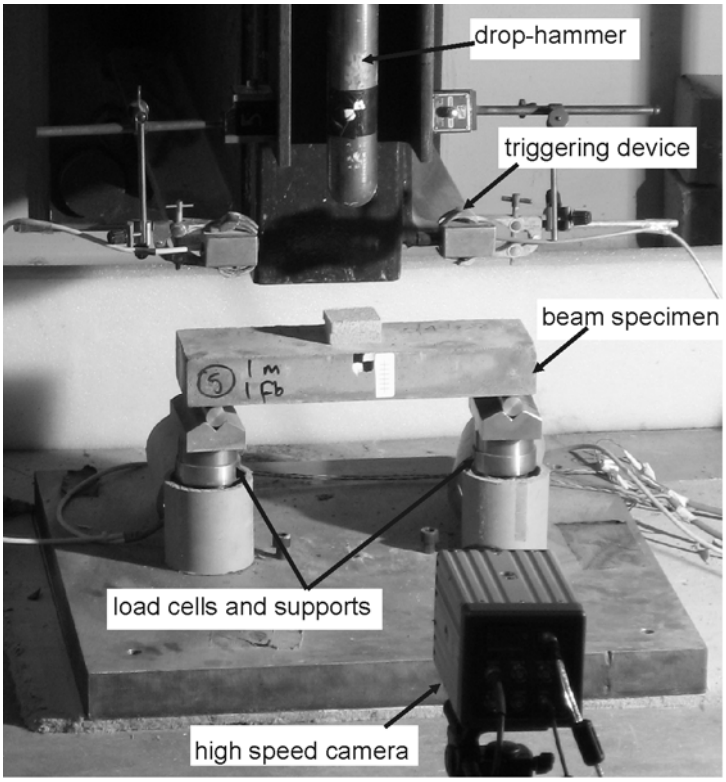

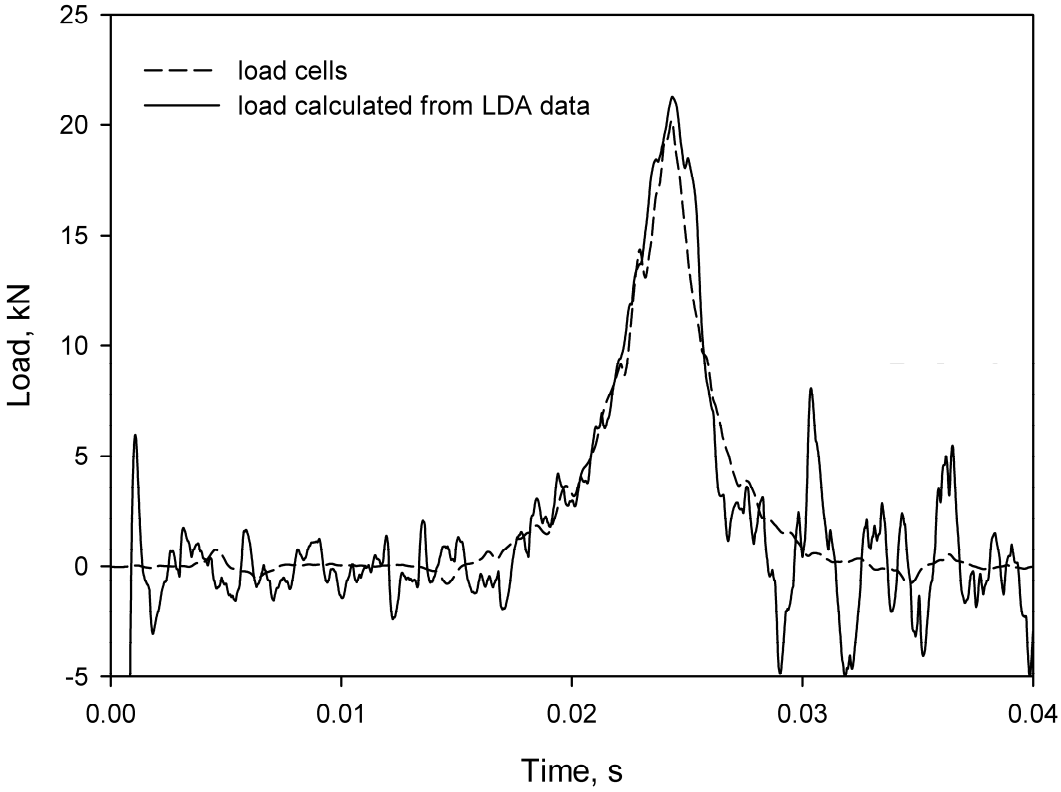
load cells
load calculated from LDA data
Load, kN
Time, s
25
20
15
10
5
0
-5
0.00
0.01
0.02
0.03
0.04

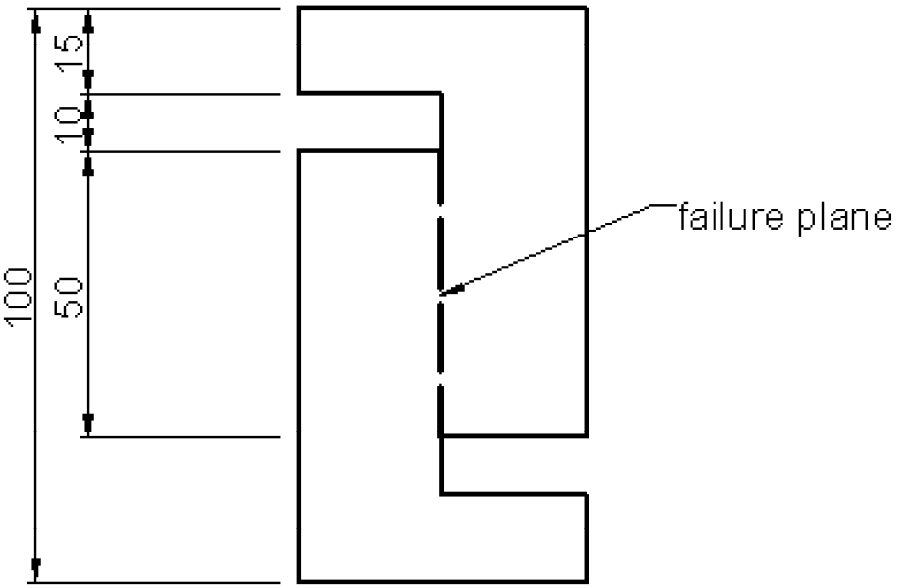

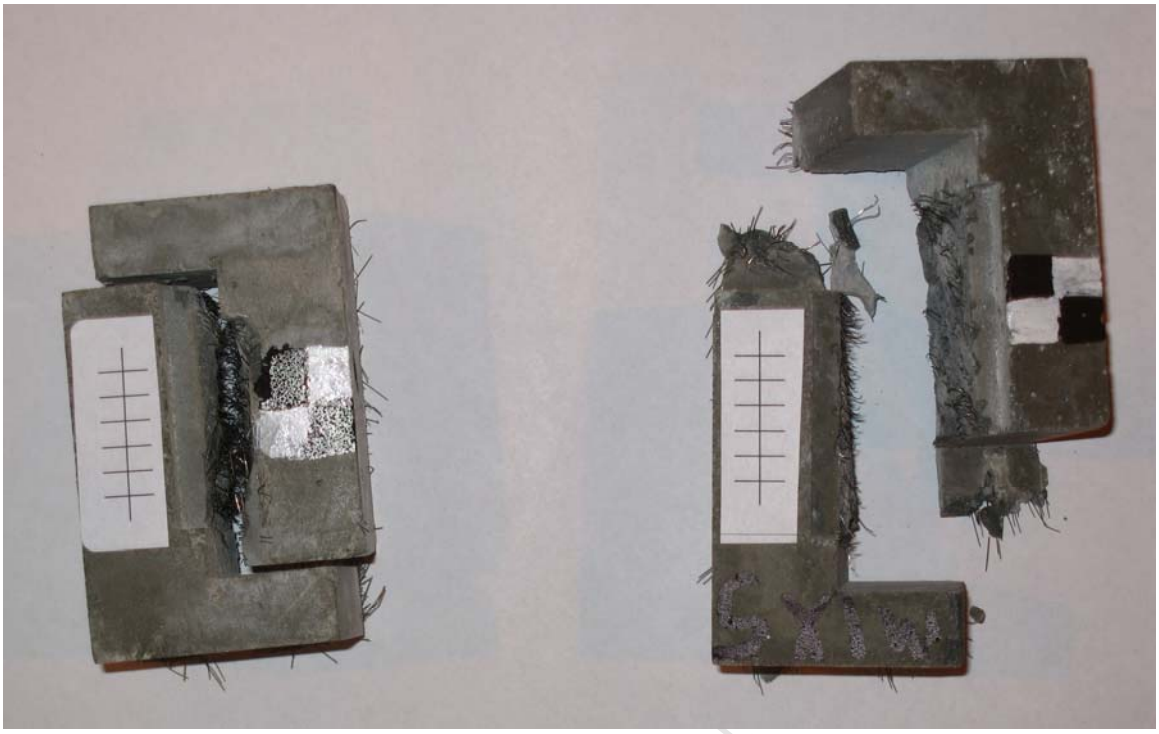

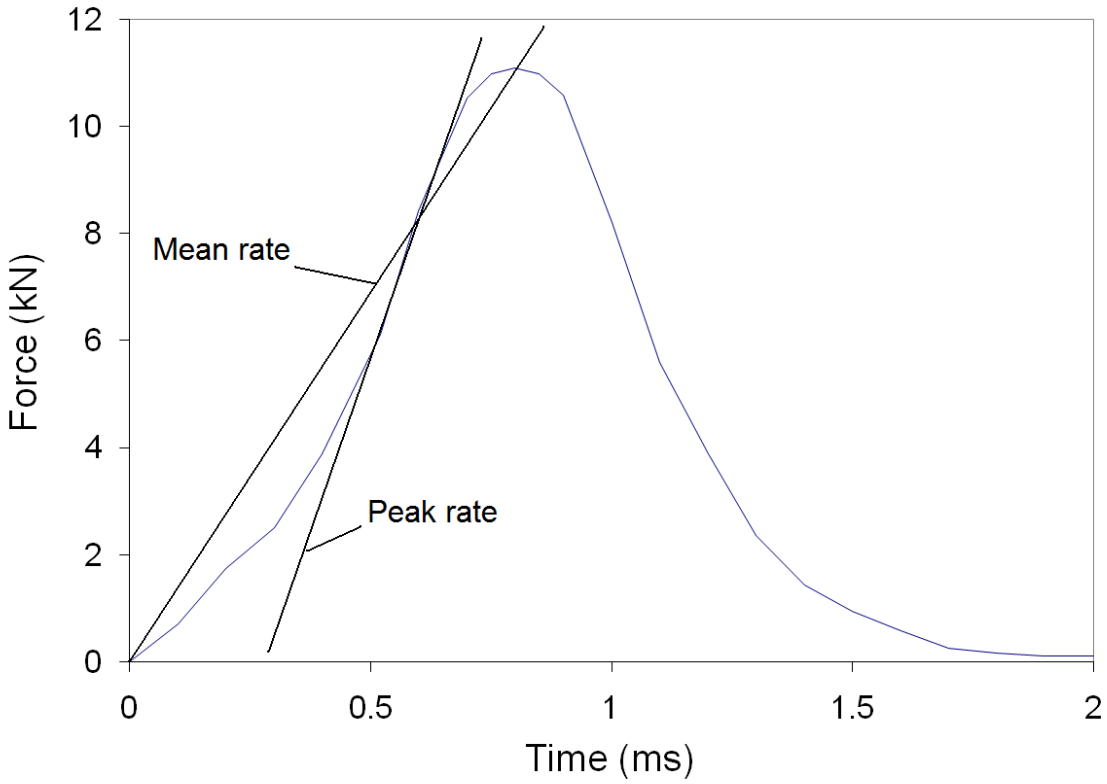

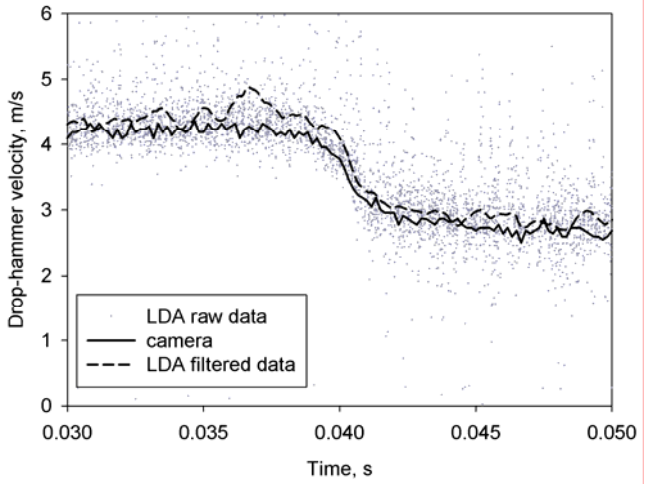

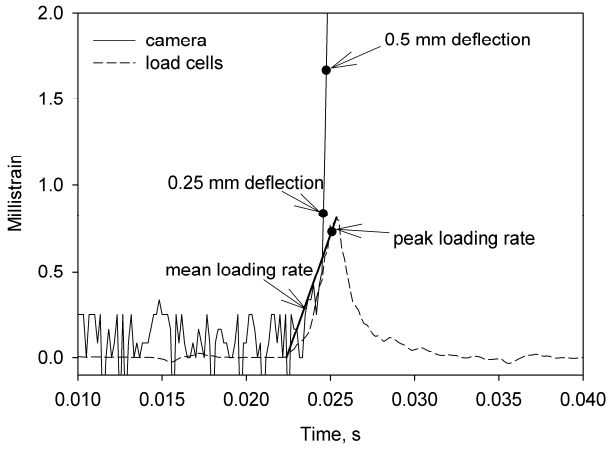

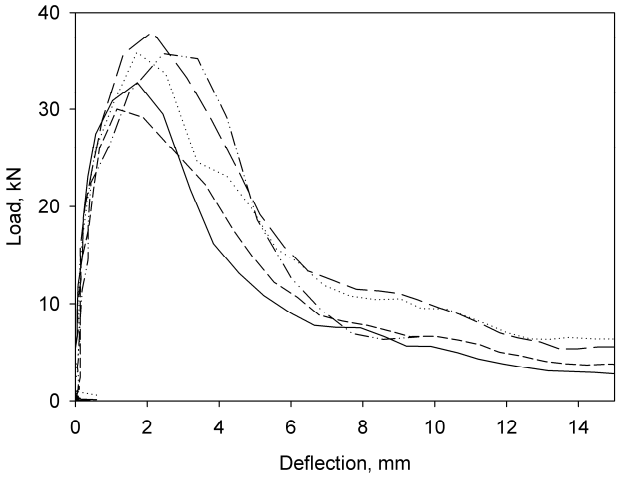

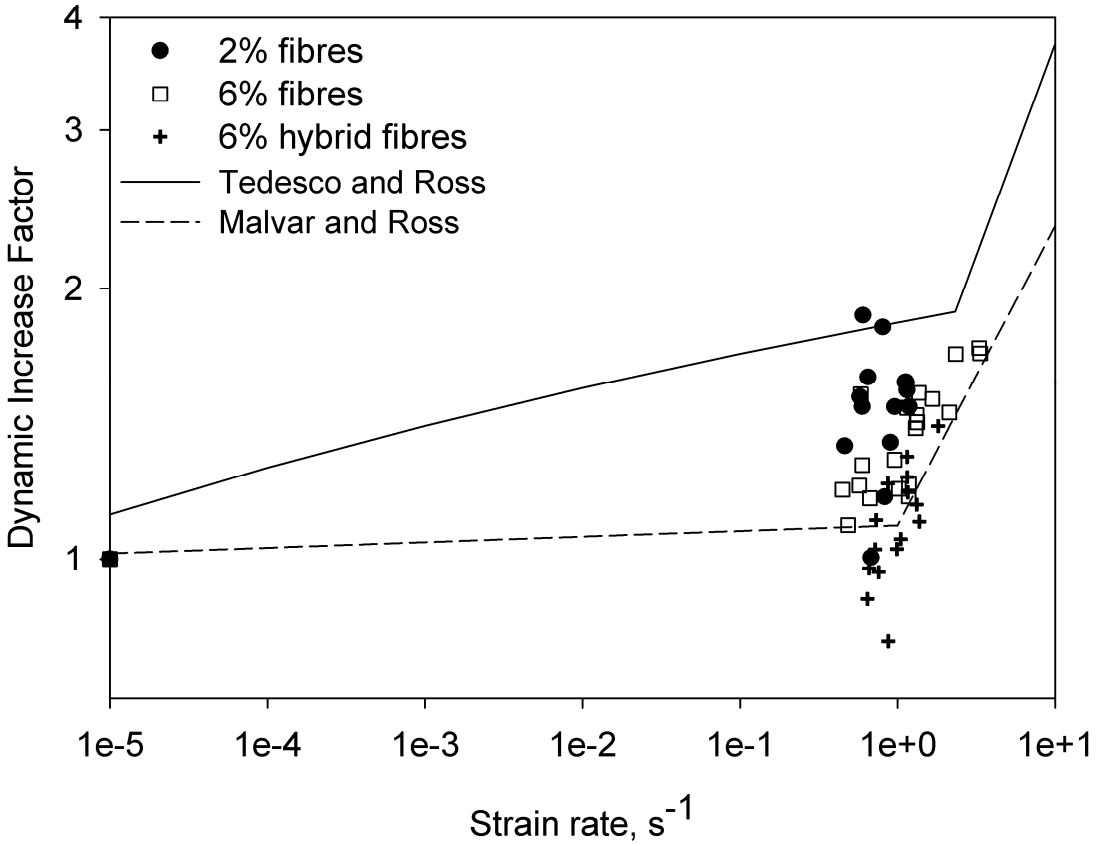
4
3
2
1
Dynamic Increase Factor
2% fibres
6% fibres
6% hybrid fibres
Tedesco and Ross
Malvar and Ross
1e-5
1e-4
1e-3
1e-2
1e-1
1e+0
1e+1
Strain rate, s-1

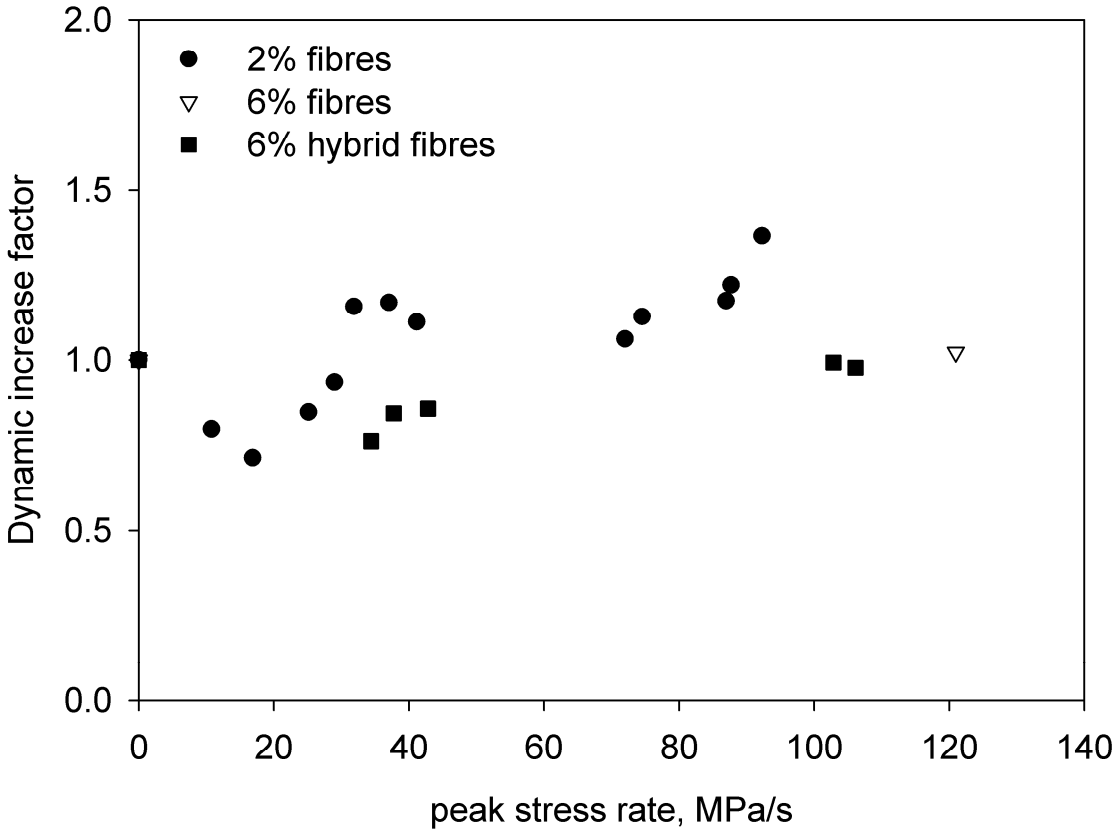
2% fibres
6% fibres
6% hybrid fibres
Dynamic increase factor
peak stress rate, MPa/s
0.0
0.5
1.0
1.5
2.0
0
20
40
60
80
100
120
140

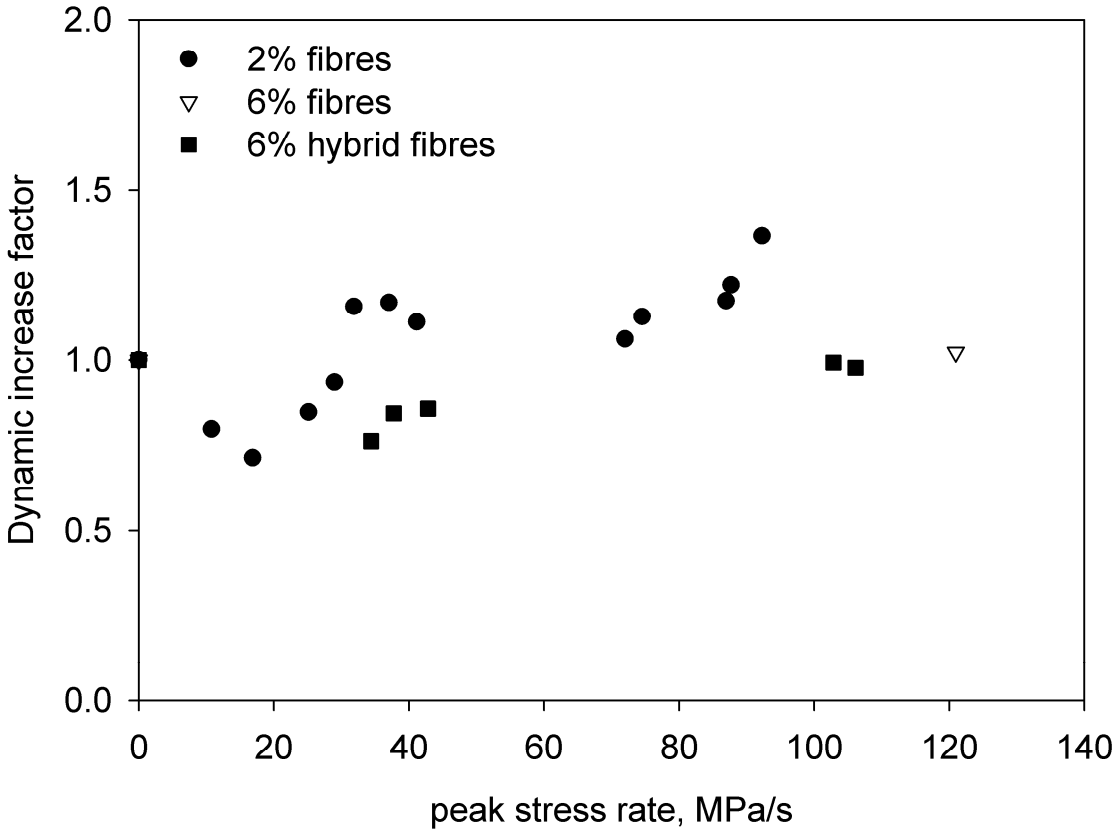
2% fibres
6% fibres
6% hybrid fibres
Dynamic increase factor
peak stress rate, MPa/s
0.0
0.5
1.0
1.5
2.0
0
20
40
60
80
100
120
140